J. Phys. Chem. B 2000, *104*, 8836−8840

Super-Repellent Composite Fluoropolymer Surfaces

S. R. Coulson, I. Woodward, and J. P. S. Badyal*

Department of Chemistry, Science Laboratories, Durham University, Durham DH1 3LE, England, U.K.

S. A. Brewer and C. Willis

DERA, Porton Down, Salisbury SP4 0JQ, England, U.K.

Received: January 4, 2000; In Final Form: April 17, 2000

Deposition of low surface energy plasma polymer layers onto microroughened PTFE substrates is found to give rise to high repellency toward polar and nonpolar probe liquids. This behavior has been interpreted in terms of Wenzels theory and the Cassie−Baxter relationship.

1. Introduction

Liquid repellency of solid surfaces is critical for many applications; these include the prevention of icing in cold weather,[1] stopping clotting in artificial blood vessels,[2] and stain-resistant textiles.[3] In this context, poly(tetrafluoroethylene) (PTFE) is considered to be the "benchmark" low surface energy material, displaying water repellency[4] in combination with other desirable properties such as high thermal stability, chemical inertness and a low coefficient of friction.[5] However, PTFE has limitations in that it exhibits poor repellency toward low surface tension liquids such as oils. One way to improve liquid repellency is to combine chemical and geometric factors;[6,7] previous attempts have included fractal surfaces,[8] functionalization of roughened substrates with perfluoroalkyl groups,[9,10] compression of submicron diameter PTFE spheres,[11,12] plasma deposition in the powder regime,[13−18] and others.[19,20] A new approach is described in this article comprising plasmachemical roughening of PTFE substrates followed by the deposition of low surface energy plasma polymer layers. X-ray photoelectron spectroscopy (XPS), atomic force microscopy (AFM), and contact angle analysis have been used to rationalize the observed enhancement in liquid repellency.

2. Experimental Section

Two types of PTFE substrate were employed in these studies: flat sheet (Goodfellow, 0.25 mm thickness), and porous film (Tetratex, 50 μm thickness, 0.1 μm pore size). Plasma treatments were carried out in an inductively coupled cylindrical reactor (5 cm diameter, 470 cm^3 volume, base pressure of 6×10^{-3} mbar, and a leak rate[21] of better than 6×10^{-9} mol s^{-1}). This was connected to a thermocouple pressure gauge and a gas/monomer inlet, and pumped by a two-stage Edwards rotary pump through a liquid nitrogen cold trap. A matching L−C circuit was used to minimize the standing wave ratio (SWR) between a 13.56 MHz rf power supply and the electrical discharge. Prior to each experimental run, the reactor was scrubbed with detergent, rinsed in isopropyl alcohol, and finally oven dried. The system was then reassembled and cleaned further with a 50 W air plasma for 30 min. Next, a 3 cm × 3 cm piece of PTFE substrate was placed into the center of the reactor, and either 0.2 mbar of oxygen gas (BOC 99.5% purity, flow rate = 1 cm^3 min^{-1}) was introduced for plasma roughening, or 0.1 mbar of 1*H*,1*H*,2*H*,2*H*-heptadecafluorodecyl acrylate vapor (Fluorochem, 98% purity, further purified using multiple freeze−thaw cycles, flow rate $\approx 1.4 \times 10^{-9}$ kg s^{-1}) was used for coating deposition. After 5 min of purging, the electrical discharge was ignited. Upon termination of surface modification/deposition, the gas/monomer vapor was allowed to continue to pass over the substrate for a further 5 min, prior to venting to atmosphere. In the case of pulsed plasma polymerization of 1*H*,1*H*,2*H*,2*H*-heptadecafluorodecyl acrylate, the rf power supply was triggered by a signal generator and monitored using a cathode ray oscilloscope. The peak power (P_p = 40 W), pulse on-period (τ_{on} = 20 μs), and pulse off-period (τ_{off} = 20 000 μs) for plasma polymer deposition had been optimized in a previous study[22,23] to yield a critical surface energy on a flat glass substrate of $\gamma_c = 4.3$ mN m^{-1}.

A VG ESCALAB MKII electron spectrometer fitted with a nonmonochromated Mg Kα X-ray source (1253.6 eV) and a hemispherical analyzer operating in the CAE mode (20 eV pass energy) was used for X-ray photoelectron spectroscopy (XPS) analysis. The photoelectrons were collected at a take-off angle of 30° from the substrate normal, which corresponds to a sampling depth of approximately 10−15 Å for the C(1s) peak. XPS envelopes were fitted using a Marquardt minimization computer program with linear background subtraction and fixed width Gaussian peak shapes.[24] Elemental concentrations were calculated using instrument sensitivity factors determined from chemical standards, where C(1s):O(1s):F(1s) equals 1.00:0.36:0.23, respectively. X-ray beam damage was found to cause less than 1% change in the F:C ratio during a typical XPS scan. This was sufficiently small that no change in the C(1s) envelope was discernible.

A Digital Instruments Nanoscope III atomic force microscope was used to examine the physical structure of the plasma-modified surfaces. The microscope was operated in tapping mode. Where changes in the oscillation amplitude of the cantilever tip serve as a feedback signal for measuring topo-

* To whom correspondence should be addressed.

10.1021/jp0000174 CCC: $19.00
Published on Web 08/22/2000

TABLE 1: Probe Liquid Contact Angles for Flat and Porous PTFE Substrates[a]

	contact angle/deg			
	water		decane	
treatment	flat	porous	flat	porous
untreated	116 ± 2	146 ± 1	46 ± 2	wicks
O_2 plasma	131 ± 4	153 ± 2	55 ± 2	wicks
plasma polymer	121 ± 3	144 ± 1	83 ± 1	115 ± 1
O_2 plasma + plasma polymer	148 ± 1	152 ± 1	92 ± 3	133 ± 2

[a] Oxygen plasma treatment was carried out at 50 W for 5 min. The error values represent the standard deviation obtained from five measurements.

graphic variations across a surface.[25] All of the AFM images were acquired in air and are presented as unfiltered data. Root-mean-square (rms) roughness values were obtained from 10 μm × 10 μm images.[26]

Sessile drop contact angle measurements were carried out at 20 °C using video capture apparatus in combination with a motorized syringe (A.S.T. Products VCA2500XE). The contact angle image was acquired within 15 s of dispensing a 2 μL size liquid drop, and then checked after 60 s for any relaxation. No reduction in volume was evident over these time scales, except for the wicking behavior reported in Table 1. Purified water (B.S. 3978 grade 1) and decane (Aldrich) were used as the probe liquids.

3. Theory

When a drop of liquid rests on a surface, unless spreading takes place, the liquid−vapor interface will form a finite angle (θ) with the assumed planar solid surface.[27] The relationship between the surface tension, γ, and the contact angle, θ, is given by Young's equation;[28]

$$\gamma_{sv} - \gamma_{sl} = \gamma_{lv} \cos \theta \qquad (1)$$

where γ_{sv}, γ_{sl}, and γ_{lv} are the surface energies of the solid−vapor, solid−liquid, and the liquid−vapor interfaces, respectively. However, such surfaces are rarely smooth in practice, and the effect of roughness must be considered.

If the surface is microscopically rough (but not so rough as to form voids at the solid−liquid interface), then the roughness factor r (defined as the ratio of true surface area compared to projected surface area) can be taken into account using the Wenzel equation:[6,29]

$$\cos \theta_W = r \cos \theta_Y \qquad (2)$$

where the subscripts W and Y correspond to the Wenzel and Young angles, respectively. Since the roughness is always greater than 1, it can be seen that roughness will accentuate the wetting/repellency behavior of a solid; i.e., if the intrinsic contact angle for a liquid on a solid surface is less/greater than 90°, roughening the surface will reduce/increase the contact angle, thereby promoting liquid wetting/repellency in accordance with eq 2.

However, if there is sufficient roughness for air to become trapped in the voids between the solid and liquid to form a composite interface, then Cassie and Baxter's (CB) extension of Wenzel's theory is more appropriate.[30] The contact angle is now given by

$$\cos \theta_{CB} = f_{sl} \cos \theta_Y - f_{la} \qquad (3)$$

where f_{sl} and f_{la} are the fractional coverages corresponding to the solid−liquid and liquid−air interfacial areas. In this case, the depth of the crevices at the surface does not alter the contact angle, and therefore the width of the aspirates and the distance between them are the critical parameters.

Comparison of the Cassie−Baxter equation with the Wenzel equation shows that the main difference between composite (air trapped) and rough surfaces is that for most finite contact angle values; the former predicts greater contact angles relative to the corresponding smooth surface, whereas this only holds true in the latter case when contact angles exceed 90° contact angle on the flat substrate (i.e., less than 90° on a smooth surface gives rise to a smaller contact angle upon roughening).[31]

Finally, in the case of very rough/porous surfaces, and depending upon the surface tension of the probe liquid, wetting can shift from an interfacial phenomena to a capillary effect culminating in wicking.[32,33]

4. Results and Discussion

Water has a higher surface tension (γ = 72.8 mN m^{-1}) compared to decane (γ = 23.8 mN m^{-1}) and therefore it exhibits a larger contact angle on flat PTFE (γ_c = 18.5 mN m^{-1}).[34−36] An increase in water contact angle is observed on going to the porous PTFE substrate[37] in accordance with the Cassie−Baxter relationship[30] (Table 1), whereas the lower surface tension decane spreads out, probably as a consequence of capillary phenomenon into the large pores.[32,33]

Oxygen plasma treatment is known to microroughen PTFE without perturbing its chemical identity.[38,39] This occurs as a consequence of ions and high-energy photons from the electrical discharge impinging upon the polymer surface to generate free radical sites, which then react with atomic or molecular oxygen, followed by polymer chain scission.[40,41] AFM confirmed that surface roughening takes place (Figure 1), while XPS verified the absence of any chemical change at the surface,[42] since only the characteristic $\underline{CF}_2$ peak at 291.2 eV, and its corresponding Mg K$\alpha_{3,4}$ satellite peak shifted by ~9 eV toward lower binding energy[43] were present (Figure 2). Oxygen plasma surface roughening produced a corresponding rise in water contact angle[38,44−46] for both types of PTFE substrate (although there is no variation in the critical surface tension of the PTFE substrate[47]) (Figure 3). Both electrical discharge power and duration of plasma exposure were found to influence the water contact angle. Oxygen plasma treatment at 50 W for 5 min was chosen as the optimum conditions for the remaining studies. The increase in decane contact angle for the flat PTFE substrate suggests that sufficient surface roughening occurs in order to produce an air−PFTE composite surface which obeys the Cassie−Baxter relationship,[31] rather than just a mere increase in interfacial area, which according to Wenzel's relationship would have led to a decrease in contact angle (since the contact angle of decane is less than 90° on flat PTFE)[48] (Table 1). In the case of the porous PTFE substrate, capillary action persists for decane even after oxygen plasma roughening.

Deposition of approximately a 10 nm layer of 1*H*,1*H*,2*H*,2*H*-heptadecafluorodecyl acrylate pulsed plasma polymer onto the flat and porous PTFE substrates gave rise to an improvement in repellency for both probe liquids. This can be attributed to the long perfluorocarbon chains contained in the plasma polymer structure having a lower surface energy compared to PTFE (γ_c = 6.0 and 18.5 mN m^{-1}, respectively).[34,35] It is of particular interest to note that the high decane contact angle measured for the coated flat PTFE surface is now sufficient to prevent

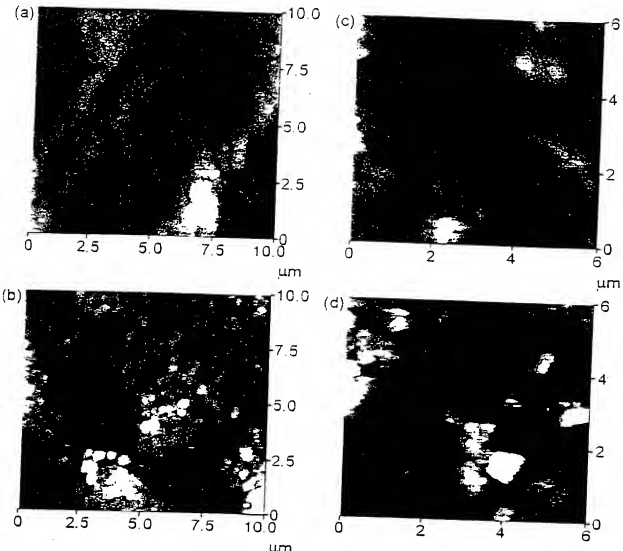

Figure 1. AFM images of (a) untreated flat PTFE substrate, rms roughness = 97 nm, z scale = 0.5 µm; (b) following oxygen plasma treatment of flat PTFE substrate for 5 min at 50 W, rms roughness = 321 nm, z scale = 2.0 µm; (c) untreated porous PTFE substrate, rms roughness = 202 nm, z scale = 2 µm; (d) following oxygen plasma treatment of porous PTFE substrate for 5 min at 50 W, rms roughness = 486 nm, z scale = 2 µm. Deposition of a 10 nm liquid repellent plasma polymer layer produced no changes in topography on the scale shown.

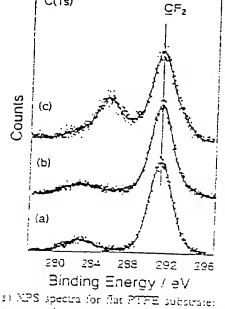

Figure 2. C(1s) XPS spectra for flat PTFE substrates: (a) untreated, (b) following oxygen plasma treated for 5 min at 50 W, and (c) deposition of pulsed perfluorocarbon onto acrylate onto (a).

capillary action into the porous PTFE substrate. The possibility of the plasma-deposited coating sealing off the pores was checked by using lower surface tension probe liquids. Hexane was found to wick in, and hence the pores had not been blocked by plasma polymer. Therefore, the enhancement in decane contact angle must be due to liquid repellency. This is consistent with the pore size (100 nm) being far greater than the thickness of the plasma polymer layer (10 nm). He gas permeability measurements[30] confirmed the absence of pore blockage.

The chemical nature of the deposited plasma polymer layer was checked by fitting the C(1s) XPS spectra to 7 Mg $K\alpha_{1,2}$ components:[31,32] $\underline{C}_xH_y$ at 285.0 eV, $\underline{C}$—C(O)=O at 285.7 eV, $\underline{C}$—O/$\underline{C}$—CF_n at 286.6 eV, $\underline{C}F$ at 287.8 eV, O—$\underline{C}$=O/$\underline{C}F$—CF_n at 289.0 eV, $\underline{C}F_2$ at 291.2 eV, and $\underline{C}F_3$ at 293.3 eV (there are also corresponding Mg $K\alpha_{3,4}$ satellite peaks shifted by ~9 eV toward lower binding energy[32]). On this basis, 46.7 ± 0.5% of the surface consisted of $\underline{C}F_2$ groups, and 14.6 ± 1.3% was $\underline{C}F_3$. The remaining oxygenated/hydrogenated carbon centers originate from the acrylate functionality contained in the monomer.[33]

Oxygen plasma roughening of the PTFE substrates followed by pulsed plasma polymer deposition gave rise to a further enhancement in the water and decane contact angles; with porous PTFE yielding the best values (Table 1 and Figure 4). This can be attributed to the combined effect of the micro-roughened air—polymer composite interface and the low surface energy nature of the plasma polymer layer. The observed increase in decane contact angle, despite it being less than 90°

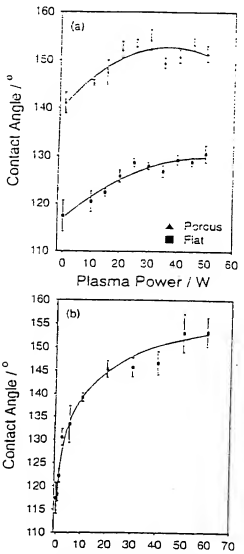

Figure 3. Water contact angle for flat and porous PTFE substrate following oxygen plasma treatment as a function of (a) electrical discharge power for 2 min; and (b) treatment time at 50 W (the porous PTFE membrane was restricted to short exposures due to its fragile nature). Lines of best fit are shown, and the error bars represent the standard deviation obtained from five measurements.

Figure 4. Photograph of 5 μL water droplet placed on the porous PTFE substrate which has been oxygen plasma treated for 5 min at 50 W and then coated with the long perfluorocarbon chain acrylate pulsed plasma polymer.

for the plasma polymer coated flat PTFE surface, is consistent with the Cassie–Baxter theory for composite interfaces wherein the Wenzel relationship would have predicted a decrease in contact angle).[31,48] Similar behavior for low surface tension liquids has been observed upon roughening other types of substrate which form composite interfaces.[22,24] In fact, the decane contact angle obtained for the plasma polymer coated microroughened porous PTFE substrate appears to be greater than most other reported oil repellent systems.[10,47,53–64]

5. Conclusions

Oxygen plasma microroughening of nonporous and expanded PTFE substrates enhances water repellency. However, lower surface tension liquids such as decane wick out on porous PTFE as a consequence of capillary action. Deposition of a low surface energy plasma polymer coating on top of these microroughened PTFE surfaces further improves liquid repellency, with decane no longer penetrating into the subsurface of the expanded PTFE substrate as a consequence of the greater contact angle formed at the liquid–solid interface. Wenzel's theory does not appear to stand up for this experimental system, whereas the Cassie–Baxter relationship is more appropriate.

Acknowledgment. S.R.C. would like to thank DERA for a Ph.D. studentship.

References and Notes

(1) Saito, H.; Takai, K.-I.; Yamauchi, G. *Mater. Sci. Res. Internat.* **1997**, *3*, 185.
(2) Busscher, H. J.; Stokroos, I.; Van der Mei, H. C.; Rouxhet, P. G.; Schakenraad, J. M. *J. Adhes. Sci. Technol.* **1992**, *6*, 347.
(3) Kissa, E. In *Handbook of Fibre Science and Technology*; Lewin, M., Sello, S. B., Eds.; Marcel and Dekker Inc.: New York, 1984; p 143.
(4) Wu, S. *Polymer Interface and Adhesion*; Marcel Dekker: New York, 1982.
(5) Feiring, A. E.; Imbalzano, J. F.; Kerbow, D. L. *Adv. Fluoroplast. Plast. Eng.* **1994**, 27.
(6) Wenzel, R. W. *Ind. Eng. Chem.* **1936**, *28*, 988.
(7) Hazlett, R. D. *J. Colloid Interface Sci.* **1990**, *137*, 527.
(8) Onda, T.; Shibuichi, S.; Satoh, N.; Tsujii, K. *Langmuir* **1996**, *12*, 2125.
(9) Ogawa, K.; Soga, M.; Takada, Y.; Nakayama, I. *Jpn. J. Appl. Phys.* **1993**, *32*, 614.
(10) Clark, J. C.; Debe, M. K.; Johnson, H. E.; Ross, D. L.; Schultz, R. K. Int. Pat. No. WO 96/34697, 7th November 1996.
(11) Chen, W.; Fadeev, A. Y.; Hsieh, C.; Oner, D.; Youngblood, J.; McCarthy, T. J. *Langmuir* **1999**, *15*, 3395.
(12) Saito, H.; Takai, K.; Yamauchi, G. *Surf. Coat. Int.* **1997**, *4*, 168.
(13) Chen, W.; Fadeev, A. Y.; Hsieh, C.; Oner, D.; Youngblood, J.; McCarthy, T. J. *Langmuir* **1999**, *15*, 3395.
(14) Saro, D.; Jikei, M.; Kakimoto, M.-A. *Polym. Prepr. (Am. Chem. Soc., Div. Polym. Chem.)* **1998**, *39*, 926.
(15) Takai, O.; Hozumi, A.; Inoue, Y.; Komori, T. *Buil. Mater. Sci.* **1997**, *20*, 817.
(16) Hozumu, A.; Takai, O. *Thin Solid Films* **1997**, *303*, 222.
(17) Sasaki, H.; Shouji, M. *Chem. Lett.* **1998**, 293.
(18) Veeramasuneni, S.; Drelich, J.; Miller, J. D.; Yamauchi, G. *Prog. Organic Coatings* **1997**, *31*, 265.
(19) Groning, P.; Schneuwly, A.; Schlapbach, L. *J. Vac. Sci. Technol.* **1996**, *A14*, 3045.
(20) Sigurdsson, S.; Shishoo, R. *J. Appl. Polym. Sci.* **1997**, *66*, 1591.
(21) Enrlich, C. D.; Basford, J. A. *J. Vac. Sci. Technol.* **1992**, *A10*, 1.
(22) Coulson, S. R.; Brewer, S.; Willis, C.; Badyal, J. P. S. *Chem. Mater.* **2000**, *12*, 2051.
(23) Coulson, S. R.; Brewer, S.; Willis, C.; Badyal, J. P. S. GB Pat. 9917 Appl. No. 9712338.4.
(24) Evans, J. F.; Gibson, J. H.; Moulder, J. F.; Hammond, J. S.; Goretzki, H. *Fresenius J. Anal. Chem.* **1984**, *319*, 841.
(25) Chong, M.; Inniss, D.; Kohler, K.; Illings, V. B. *Surf. Sci.* **1993**, *290*, L688.
(26) ASTM B46[1]-94 ASTM-ISO recommended recommendation for analyzing and reporting surface roughness.
(27) Cherry, B. W. In *Aspects of Surface Chemistry and Morphology in Plastics-Surface and Finish*; Pinner, S. H., Simpson, W. G., Eds.; Butterworths: London, 1971.

(23) Young, T. *Philos. Trans R. Soc. London* 1805, *95*, 65.
(29) Wenzel, R. N. *J. Phys. Chem.* 1949, *53*, 1466.
(30) Cassie, A. B. D.; Baxter, S. *Trans. Faraday Soc.* 1944, *40*, 546.
(31) Meillet, J. L. *Water Proofing and Water Repellency*; Elsevier: London, 1963; p 28.
(32) Adamson, A. W. *Physical Chemistry of Surfaces*, 5th ed.; Wiley: New York, 1990; p 495.
(33) Garbassi, F.; Morra, M.; Occhiello, E. *Polymer Surfaces: From Physics to Technology*; John Wiley and Sons: Chichester, UK, 1994; p 183.
(34) Fox, H. W.; Zisman, W. A. *J. Colloid Sci.* 1950, *5*, 514.
(35) Jasper, J. J. *J. Phys. Chem. Ref. Data* 1972, *1*, 841.
(36) Dalal, E. N. *Langmuir* 1987, *3*, 1009.
(37) Tröger, J.; Lunkwitz, K.; Bürger, W. *J. Colloid Interface Sci.* 1997, *194*, 281.
(38) Morra, M.; Occhiello, E.; Garbassi, F. *Surf. Interface Anal.* 1990, *16*, 412.
(29) Ryan, M. E.; Badyal, J. P. S. *Macromolecules* 1995, *28*, 1377.
(40) Smolinsky, G.; Vasile, M. J. *Eur. Polym. J.* 1979, *15*, 37.
(41) Egitto, F. D.; Matienzo, L. J.; Schreyer, H. B. *J. Vac. Sci. Techol.* 1992, *10*, 3060.
(42) Badev, J. P.; Urbaczewski-Espuche, E.; Jugnett, Y.; Sage, D.; Duc, T. M.; Chabert, B. *Polym.* 1994, *35*, 2472.
(43) Briggs D.; Seah M. P. *Practical Surface Analysis by Auger and X-ray Photoelectron Spectroscopy*; John Wiley and Sons: Chichester, England, 1983.
(44) Morra, M.; Occhiello, E.; Garbassi, F. *Langmuir* 1989, *5*, 872.
(45) Golub, M. A.; Wydeven, T.; Cormua, R. D. *Langmuir* 1991, *7*, 1026.
(46) Morra, M.; Occhiello, E.; Garbassi, F. *Langmuir* 1989, *5*, 872.
(47) Chen, J.-R.; Wakida, T. *J. Appl. Polym. Sci.* 1997, *63*, 1733.
(48) Drelich, J.; Miller, J. D.; Good, R. J. *J. Colloid Interface Sci.* 1996, *179*, 37.
(49) Johnson, R. E.; Dettre, R. H. *Polym. Prepr. (Am. Chem. Soc., Div. Polym. Chem.)* 1987, *28*, 48.
(50) Barker, C. P.; Kochem, K. H.; Revell, K. M.; Kelly, R. S. A.; Badyal, J. P. S. *Thin Solid Films* 1995, *259*, 46.
(51) Clark, D. T.; Shuttleworth, D. *J. Polym. Sci. Chem. Ed.* 1980, *18*, 27.
(52) Beamson, G.; Briggs, D. *High-Resolution XPS of Organic Polymers, The Scienta ESCA300 Database*; John Wiley and Sons: Chichester, England, 1992.
(53) Minami, T.; Katata, N.; Tadanaga, K. *SPIE* 1997, *3136*, 168.
(54) Shibuichi, S.; Yamamoto, T.; Onda, T.; Tsujii, K. *J. Colloid Interface Sci.* 1998, *208*, 287.
(55) Balkenende, A. R.; van de Boogaard, H. J. A. P.; Scholten, M.; Willard, N. P. *Langmuir* 1998, *14*, 5907.
(56) Thomas, R. R.; Anton, D. R.; Graham, W. F.; Darmon, M. J.; Stika, K. M. *Macromolecules* 1998, *31*, 4595.
(57) Park, I. J.; Lee, S. B.; Choi, C. K.; Kim, K. J. *J. Colloid Interface Sci.* 1996, *181*, 284.
(58) Schmidt, D. L.; Coburn, C. E.; DeKoren, B. M.; Potter, G. E.; Meyers, G. F.; Fischer, D. A. *Nature* 1994, *368*, 39.
(59) Anton, D.; Thomas, R.; Kirchner, J. *Polym. Prepr. (Am. Chem. Soc., Div. Polym. Chem.)* 1998, *39*, 954.
(60) Sawada, H.; Ohashi, A.; Oue, M.; Baba, M.; Abe, M.; Mitani, M.; Nakajima, H. *J. Fluorine Chem.* 1995, *75*, 121.
(61) Thunemann, A. F.; Lochhaas, K. H. *Langmuir* 1999, *15*, 4867.
(62) Thunemann, A. F.; Lieske, A.; Paulke, B. R. *Adv. Mater.* 1999, *11*, 321.
(63) Hopken, J.; Moller, M. *Macromolecules* 1992, *25*, 1461.
(64) Kobayashi, H. *Makromol. Chem.* 1993, *194*, 2569.